PCCP

RSC Publishing

Factors affecting the selectivity of the photocatalytic conversion of nitroaromatic compounds over TiO₂ to valuable nitrogen-containing organic compounds†

Amer Hakki, Ralf Dillert and Detlef W. Bahnemann*

The photocatalytic conversion of various nitroaromatic compounds in alcohols employing four different types of TiO₂ (Sachtleben Hombikat UV100 as anatase, Crystal Global R34 as rutile, Evonik-Degussa Aeroxide P25 as an anatase–rutile mixture, and home-made mesoporous anatase) has been studied. The effect of platinization of these different types of TiO₂ on the reaction sequence has also been investigated. Upon irradiation of an ethanolic solution of *m*-nitrotoluene, as a model reaction, in the presence of the bare photocatalyst, different products were obtained according to the applied photocatalyst. It was found that the surface properties of the photocatalyst play an important role in the reaction pathway and thus in the selectivity of the products. In all cases, a simultaneous reduction of the nitro compound and an oxidation of the alcohol are induced by the photogenerated electrons and holes, respectively. An imine is then produced upon condensation of the generated aldehyde and amino compounds. Rutile was found to be more selective towards the primary amino compound (*m*-toluidine) while anatase catalysts gave a mixture of *m*-toluidine and its imine (*N*-ethylidene-3-methylaniline). A cyclization reaction of the produced imine to generate methyl quinoline was observed when Aeroxide P25 was used as a photocatalyst. Employing platinized TiO₂, the hydrogenation of the produced imine yielding N-alkylated products was found to occur in all cases. However, the selectivity towards the mono N-alkylated product was the best using platinized Hombikat UV100. This selectivity was found to be also influenced by the loaded amount of Pt, the platinization method, and the illumination time but not by the light intensity.

Introduction

The use of photocatalytic methods as a promising approach for green and sustainable organic synthesis has attracted increased interest in recent years owing to their unique properties.[1–3] The photoinduced charge separation occurring on the TiO₂ surface creates both a reduction center and an oxidation center at the same time. This unique feature allows several transformations to be performed in one sequence without the necessity of the isolation of the intermediates.[4–8] Furthermore, these redox reactions by photogenerated electrons and holes do not produce by-products usually originating from the reductant or the oxidant; this is contrastive to conventional redox reagents such as permanganate or lithium aluminum hydride to leave, respectively,

manganese ion or aluminum hydroxide after oxidation and reduction. Moreover, photocatalytic organic conversions can sometimes offer higher selectivities than conventional methods.[9]

A variety of organic transformations mediated by irradiation of semiconductors has been reported including oxidation and/or reduction, and some coupling reactions.[6,7,10–12]
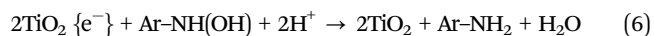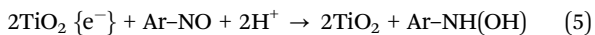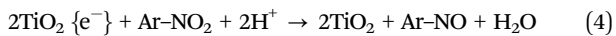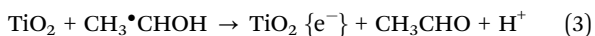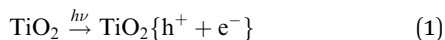
Among the photocatalytic reductions, the reduction of nitroaromatic compounds has been studied most extensively. In this case, the presence of dioxygen (O₂) must be avoided since O₂ competes with the nitroaromatic compound for electrons. Moreover, a hole scavenger is needed to avoid recombination between electrons and photogenerated holes (h⁺) within the photocatalyst particle. It is well known that primary alcohols (such as methanol or ethanol) can be used as hole scavengers and solvent in the photocatalytic reduction of nitro aromatic compounds, generating the corresponding aldehydes as oxidation products.

The photocatalytic reduction of the nitro group to the amino group on the surface of TiO₂, in the absence of oxygen and in

Institut für Technische Chemie, Leibniz Universität Hannover, Callinstr. 3, D-30167 Hannover, Germany. E-mail: Bahnemann@iftc.uni-hannover.de

† Electronic supplementary information (ESI) available. See DOI: 10.1039/c2cp44153e

2992 | *Phys. Chem. Chem. Phys.*, 2013, **15**, 2992–3002

This journal is © the Owner Societies 2013

the presence of alcohols as sacrificial electron donors, is well established and summarized in eqn (1)–(6).[13–15]

$$TiO_2 \xrightarrow{h\nu} TiO_2\{h^+ + e^-\} \quad (1)$$

$$TiO_2\{h^+\} + CH_3CH_2OH \rightarrow TiO_2 + CH_3{}^\bullet CHOH + H^+ \quad (2)$$

$$TiO_2 + CH_3{}^\bullet CHOH \rightarrow TiO_2\{e^-\} + CH_3CHO + H^+ \quad (3)$$

$$2TiO_2\{e^-\} + Ar-NO_2 + 2H^+ \rightarrow 2TiO_2 + Ar-NO + H_2O \quad (4)$$

$$2TiO_2\{e^-\} + Ar-NO + 2H^+ \rightarrow 2TiO_2 + Ar-NH(OH) \quad (5)$$

$$2TiO_2\{e^-\} + Ar-NH(OH) + 2H^+ \rightarrow 2TiO_2 + Ar-NH_2 + H_2O \quad (6)$$

Ferry and Glaze[14] suggested that the active reducing species in the TiO_2 photocatalyzed reduction of nitrobenzene with CH_3OH are not the $^\bullet CH_2OH$ radicals but the excited electrons in the conduction band (e^-_{cb}). The potential of the conduction band electrons in the anatase phase was reported[16] to be -0.908 V vs. SCE at pH = 12 which is negative enough to reduce almost all nitrobenzene derivatives (formal potentials of m-NH_2–Ph–NO_2, m-CH_3–Ph–NO_2, m-Cl–Ph–NO_2, are, respectively, -0.705, -0.705, -0.635 V vs. SCE at pH $\approx$ 12).[17]

Several reports have been published in terms of the photocatalytic conversion of nitroaromatic compounds in the presence of alcohols as hole scavengers.[5,8,13,18–23] However, these reports have shown that different products are obtained, from the system alcohol–nitroaromatic compound–TiO_2, by different groups. Mahdavi et al.[13] have reported that several nitro aromatic compounds can be effectively reduced to their corresponding amino compounds upon illumination of their ethanolic solutions in the presence of TiO_2.

On the other hand, Valenzuela and co-workers[20] have reported that illumination of alcoholic solutions of nitrobenzene over TiO_2 led to its corresponding imines with high selectivity when C1–C3 alcohols were used as solvents while a mixture of aniline and imines is produced using higher alcohols. Another example for the photocatalytic formation of imines was reported by Shiraishi et al.[21] who observed that deposition of Pt on the surface of TiO_2 promotes the selectivity towards the imine. In contrast, Ohtani et al.[18,24] have reported that secondary amines are the main products which are obtained from primary amines employing platinized titanium dioxide as a photocatalyst.[10,18,19] However, among the primary amines used in their studies, aniline was N-alkylated most slowly reaching an efficiency of only 13.9% even after 20 h of irradiation.[18] They assumed that this lower efficiency of N-alkylation of aniline is attributed to the fact that N-ethylideneaniline is poorly reduced over Pt in ethanol under an H_2 atmosphere. Matsushita et al.[25,26] have also described the photocatalytic N-alkylation process of benzylamine in a micro-reaction system with immobilized Pt-free TiO_2 as well as with Pt/TiO_2. In a previous study,[8] we reported that quinoline derivatives can be produced from the photocatalytic conversion of the nitro aromatic compounds in ethanol mediated by bare TiO_2 in the presence of an acid as a co-catalyst. The same product was also obtained by Selvam and Swaminathan[22,27,28]

although they modified the surface of TiO_2 with Pt, Au or Ag. Park et al.[5] have reported the formation of 4-ethoxy-1,2,3,4-tetrahydroquinoline upon the photocatalytic conversion of nitroaromatic compounds in ethanol.

However, in order to consider the photocatalytic reduction of the nitroaromatic compounds over TiO_2 as a useful synthetic method, a systematic study focusing on the factors that affect the selectivity of this reaction is of great importance. Herein, we investigated, for the first time, the parameters that affect the selectivity of the photocatalytic conversion of nitroaromatic compounds in alcohols towards the most valuable products such as the quinoline derivatives and the mono N-alkylated aniline derivatives. For this purpose, we have employed several kinds of TiO_2 (anatase, rutile, anatase–rutile mixture, and mesoporous anatase) in order to investigate the effect of the type of TiO_2 and its surface properties on the photocatalytic conversion of the nitroaromatic compounds in alcohols. The effect of platinization of these bare photocatalysts on the reaction pathway has also been studied. Further investigations concerning optimization of the amount of platinum loaded on the surface of TiO_2, the Pt/TiO_2 preparation method, and the light intensity, respectively, have also been carried out and are described herein. Furthermore, the scope of reactions using several nitro aromatic compounds and alcohols in the presence of platinized TiO_2 was analysed.
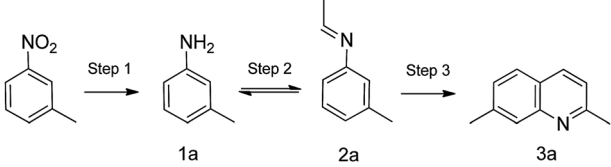
Results and discussion

A comparative study of different types of TiO_2

The conversion of m-nitrotoluene (m-NT) dissolved in ethanol was investigated as a model reaction to identify the potential of the catalysts. UV(A) irradiation ($\lambda > 320$ nm) of the photocatalyst particles suspended in an ethanolic solution of m-NT under Ar at 25 °C led to the formation of m-toluidine (1a), N-ethylidene-3-methylaniline (2a), and 2,7-dimethylquinoline (3a). However, the distribution of the products differs according to the applied photocatalyst. Table 1 summarizes the results of m-NT conversion by photoirradiation of its ethanolic solutions with the respective applied TiO_2 photocatalysts.

In all cases, the conversion of m-NT was completed after 2 h of illumination of the reaction mixtures. The GC-MS chromatograms recorded during this time indicate that the following sequence of reactions occurs: reduction of the nitro compound by the photogenerated e^- and simultaneous oxidation of the alcohol by the photogenerated h^+; imine formation; and, finally, imine cyclization (cf. scheme in Table 1).

It is clearly seen from the data shown in Table 1 that the type of TiO_2 strongly affects the distribution of the reaction products. With pure rutile (cf. entry 1 in Table 1) the main product is the corresponding aniline (1a) with a yield of 72%. On the other hand, pure anatase (cf. entries 2 and 4 in Table 1) promotes the condensation of 1a with the photocatalytically generated acetaldehyde to produce higher yield (44%) of the imine (2a). Surprisingly, P25 which is a mixture of anatase (80%) and rutile (20%) catalyses the cyclization of the imine (2a) to produce the corresponding quinoline (3a) with a good

Table 1 Results of the photocatalytic conversion of *m*-nitrotoluene in EtOH with various TiO$_2$ catalysts under UV(A) irradiation[a]

Entry	Catalyst	Notation	S_{BET}[b]/ m^2 g^{-1}	Particle size/nm	$r \times 10^8$[c]/ mol L^{-1} s^{-1}	Yields[d] (%) 1a	2a[e]	3a
1	Rutile	R	58	34	0.80	72	2	7
2	UV100	A	265	10	0.94	49	44	4
3	Aeroxide (P25)	AR	77	25	0.96	21	13	31
4	Mesoporous anatase	MA	174	13	0.70	32	44	3
5	Mix UV100 + rutile	MAR	—	A10 R34	—	48	47	5

[a] Reaction conditions: catalyst (25 mg), *m*-NT (100 μmol), EtOH (10 ml), $I > 320$ nm, 25 °C, under an Ar atmosphere. Conversions were determined by GC on the basis of *m*-NT consumption and were found to be >99% after 2 h illumination in all cases. [b] S_{BET} – surface area. [c] r – rate of the photocatalytic reduction of *m*-NT. [d] Determined by GC according to calibration curves using corresponding authentic compounds. [e] Since the authentic imine was not available, the peak area of the imine was plotted on the calibration curve of the amine assuming that both of them have the same FID signal.

yield (31%) (*cf.* entry 3 in Table 1). Mixing of anatase A with rutile R in the same ratio as that of P25 (*cf.* entry 5 in Table 1) resulted in a distribution similar to that of pure anatase indicating that the superior effect of P25 is not due to phase's mixture property. In order to understand these differences between the employed TiO$_2$ photocatalysts the BET surface areas of the different TiO$_2$ samples were measured and are presented in Table 1. However, no clear relationship between the BET surface area of the used catalyst and the distribution of the products was observed.

The observed difference in the selectivity of the photocatalytic conversion of *m*-NT using various types of TiO$_2$ can be explained by the differences in the surface properties of the applied catalysts. It is known that the difference in morphology does not only result in different textural properties (*i.e.* specific surface area and porosity) but also affects the surface structural arrangements which lead to different surface reactivity. The chemical features of the surface centers of the used photocatalysts were investigated by FTIR spectroscopy after adsorption of pyridine on their surfaces. Pyridine is one of the most selective reagents for studying the acidic sites of the solid acids.[29–32]

The FTIR absorption spectra of the pure TiO$_2$ materials, as well as of TiO$_2$ powders treated with pyridine, are shown in Fig. 1. The strong absorption peak at around 1640 cm^{-1} (Fig. 1A) is attributed to the vibrations of the surface-adsorbed H$_2$O and Ti–OH bonds. As shown in Fig. 1B, several significant new peaks at 1445, 1489, 1540, 1607, and 1639 cm^{-1} appear upon adsorption of pyridine on TiO$_2$. These peaks have been assigned to the chemisorption of molecular pyridine at different types of surface acidic sites.[33] The peaks at 1445 and 1607 cm^{-1}
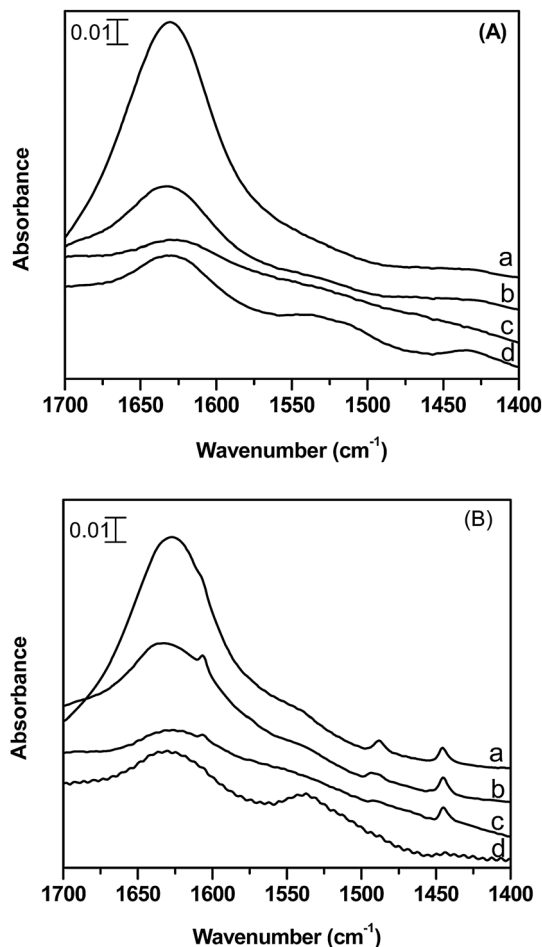
Fig. 1 Infrared spectra of bare TiO$_2$ (A) and pyridine molecules adsorbed on TiO$_2$ (B); (a) UV100, (b) P25, (c) mesoporous anatase, and (d) rutile.

are due to the interaction of pyridine with Lewis acidic sites (exposed Ti^{4+} cations), while the peaks at 1540 and 1639 cm^{-1} result from the protonation of the pyridine molecule by the Brønsted acid sites (surface-bound hydroxyl groups). However, under our experimental conditions, the peak at 1639 cm^{-1} overlapped with vibrations of the surface adsorbed water while the peak at 1540 cm^{-1} was very broad and weak. The band at 1489 cm^{-1} reflects pyridine interactions with active centers of both acid types. For the rutile sample no clear new peaks appeared after its treatment with pyridine vapor which confirms the poor acidity of this TiO$_2$ type.[29]

The acidic properties of P25, in the dark and after UV(A) irradiation, were also verified by monitoring the pyridine adsorption by ATR-FTIR (Fig. S1, ESI†). Again the adsorption bands at 1445, 1604, and 1489 cm^{-1}, which correspond to pyridine interaction with Lewis acid sites, are present in all the spectra. On the other side, the weak peak at 1640 cm^{-1}, which confirms the interaction between the pyridine molecule and the Brønsted acid sites, becomes more intensive during the UV(A) irradiation of P25 in the presence of pyridine. Several reports have also shown that P25 has both Lewis and Brønsted acid sites on its surface.[33]

These differences in the acidic properties of the employed TiO$_2$ types can explain the differences in their selectivity for the photocatalytic conversion of m-NT. Imine (**2a**) was produced in a good yield when anatase was used as a photocatalyst. The catalytic condensation of the photocatalytically produced aldehyde and amine occurs on the Lewis acid site on anatase TiO$_2$ to produce the imine (**2a**).[21] The imine was also obtained upon the dark reaction of the amine (**1a**) with 3 equiv. of acetaldehyde (the same amount of acetaldehyde that may be obtained upon reduction of 1 equiv. of the nitroaromatic compound) in the presence of Hombikat UV100 at 25 °C, which means that the photocatalytic steps are only the oxidation of the alcohol and the reduction of the nitro group.

On the other hand, the poor acidity of the rutile can explain its selectivity towards the amine (**1a**) upon the photocatalytic conversion of m-NT, whereas, the Brønsted acid sites which are available on the surface of P25 are believed to be responsible for the cyclization reaction of the produced imine, which is produced on the Lewis acid sites, to yield the corresponding quinoline (**3a**) in the presence of P25.

The importance of the Brønsted acid sites for the cyclization reactions was confirmed by direct addition of a Brønsted acid (p-toluenesulfonic acid) into the reaction dispersions containing the Hombikat UV100 as a photocatalyst. As expected, the product (**3a**) with good yield was obtained from the photocatalytic conversion of m-NT on Hombikat UV100 when the Brønsted acid

was directly added to the reaction mixture. Moreover, the GC-MS analyses showed the formation of the acetal which is believed to be an intermediate in the quinoline production. The formation of hemiacetal species from benzaldehyde mediated by P25 TiO$_2$ was also suggested in the work of Martra.[34] It is well known that acetals are formed by treatment of aldehydes with alcohols in the presence of a Brønsted acid catalyst. If the original aldehyde has an α-hydrogen, as in the case of acetaldehyde, an enol ether can be produced (see Scheme 1). Cyclization of the imine with the enol ether will lead to the formation of 4-ethoxy-2,7-dimethyl-1,2,3,4-tetrahydroquinoline which can be converted to 2,7-dimethyl-1,2-dihydroquinoline upon splitting of an alcohol molecule (see Scheme 2). Oxidation of this dihydroquinoline will, consequently, lead to the formation of 2,7-dimethyl-quinoline.[35]

Effect of platinization of TiO$_2$ on the reaction sequence

The selectivity of the products obtained after the photocatalytic conversion of m-NT using different types of TiO$_2$ modified with Pt is shown in Table 2. Table 2 shows also the selectivity of the reaction products after two and six hours of UV(A) illumination, respectively, of an ethanolic solution of m-NT in the presence of the Hombikat UV100 loaded with different amounts of Pt. The results obtained using different light intensities are also illustrated in Table 2.

It is clearly seen from the results shown in Table 2 (entries 1–8) that the presence of the co-catalyst, Pt, directs the photocatalytic reaction towards N-alkylation and N,N-dialkylation (steps 3′ and 4 in Scheme 2) of the nitro aromatic compound rather than the cyclization reaction (step 3 in Scheme 2) employing any of the TiO$_2$ types. However, steps 1 and 2 in Scheme 2 seem not to be affected by the presence or absence of Pt. In all cases, similar to the case of bare TiO$_2$, 2 h of illumination is needed to achieve 100% conversion of the starting substrate (m-NT). It is well known that the modification of the TiO$_2$ surface with Pt will enhance the photocatalytic activity because of the trapping of the photogenerated e$^-$ by Pt nanoparticles thus enhancing the charge separation between e$^-$ and h$^+$.[36] This will, in principle, accelerate the oxidation of the alcohol and the simultaneous reduction of the nitro group. However, the modification of the TiO$_2$ photocatalyst with Pt nanoparticles was not sufficient to decrease the required time to complete the m-NT reduction. This can be explained by a competition between m-NT and the
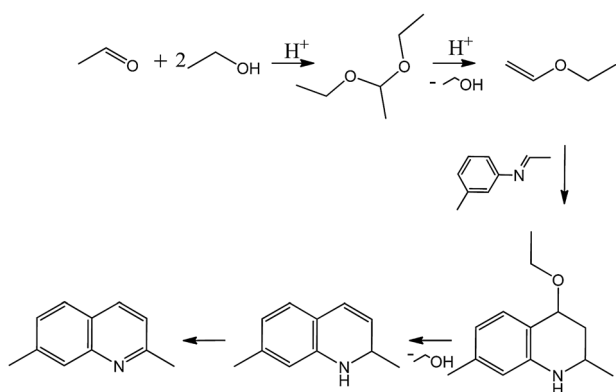
Scheme 1 Sequence of the cyclization reaction of the imine (**2a**) with EtOH via acetal formation.
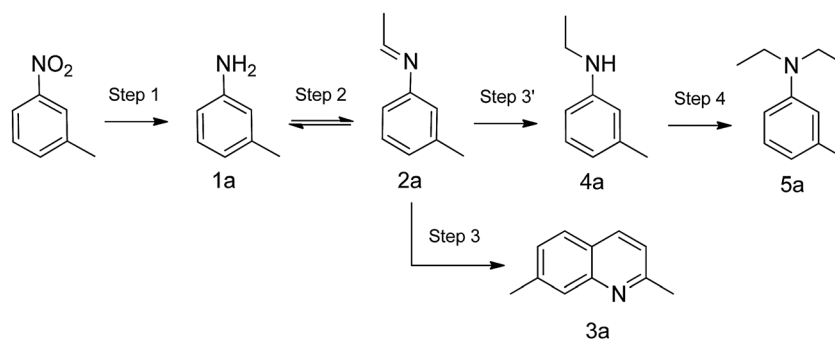
Scheme 2 Sequence of the cyclization and N-alkylation reactions of m-NT in EtOH.

Table 2 N-alkylation of m-NT with EtOH photocatalyzed by diverse Pt loaded TiO$_2$[a]

Entry[b]	Catalyst	t [h]	Conversion [%]	Selectivity[c] [%]				
				1a	2a	3a	4a	5a
1	(0.5%)Pt/A	2	100	4	4	1	69	5
2		6	100	<1	1	<1	26	59
3	(0.5%)Pt/R	2	100	13	8	7	50	7
4		6	100	3	1	4	36	43
5	(0.5%)Pt/P25	2	100	10	1	2	68	4
6		6	100	0	0	<1	43	57
7	(0.5%)Pt/MA	2	100	22	14	5	41	3
8		6	100	3	2	1	53	36
9	(0.3%)Pt/A	2	100	28	8	4	50	0
10		6	100	16	5	7	53	3
11	(1.0%)Pt/A	2	100	2	3	<1	80	5
12		6	100	<1	1	<1	35	50
13	Mix (0.5%)Pt/A	2	100	68	0	7	9	<1
14		6	100	48	0	12	22	<1
15	(0.5%)Pt/A	2	100	14	4	<1	60	<1
16	30 mW	6	100	5	2	<1	52	26
17	(0.5%)Pt/A	2	69	35	16	<1	<1	<1
18	15 mW	6	100	5	4	<1	73	8
19	(0.5%)Pt/A	2	39	48	10	<1	<1	<1
20	7.5 mW	6	100	17	10	2	43	<1
21	(0.5%)Pt/A	2	100	21	14	6	26	2
22	Ar purging	6	100	7	3	3	51	28

[a] Reaction conditions: catalyst (25 mg), m-NT (100 μmol), EtOH (10 ml), I > 320 nm, 25 °C, under an Ar atmosphere. [b] Conversions were determined by GC on the basis of m-NT consumption. [c] Determined by GC.

protons (H$^+$), which are produced by the photocatalytic oxidation of the alcohol, for the electrons trapped by Pt nanoparticles. The reduction of the protons yields molecular hydrogen which was detected only in the presence of platinized TiO$_2$ but not the bare TiO$_2$. As can be seen from Fig. 2, the rate of H$_2$ production is doubled when m-NT was replaced with 2a as a substrate. Upon illumination of an ethanolic solution of the amine (2a) in the presence of 0.5% Pt/A, about 700 μmol H$_2$ was produced within 120 min of illumination, while only 400 μmol H$_2$ was produced using m-NT as a substrate during the same time of irradiation. This means that an excess of about 300 μmol H$_2$ was observed starting from 2a as the substrate instead of m-NT. This is exactly the required amount of H$_2$ to reduce the initially present amount
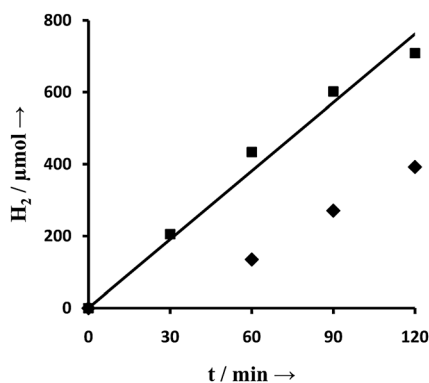

Fig. 2 H$_2$ evolution during photoirradiation of m-NT (◆) or m-AT (■) in EtOH in the presence of Pt(0.5 wt%)/TiO$_2$ as a catalyst. Reaction conditions: catalyst (25 mg), m-NT (100 μmol), EtOH (10 ml), λ > 320 nm, 25 °C, under an Ar atmosphere.

(100 μmol) of m-NT to 2a. In a reference experiment, m-NT was totally reduced to the corresponding amine (2a) when H$_2$ was purged in a reaction mixture containing 0.5% Pt/A in the dark. No reduction of the m-NT was observed under the same conditions in the dark in the presence of bare TiO$_2$. Thus, the presence of Pt as a co-catalyst may change the reducing agent of the nitro group from the conduction band electron to molecular hydrogen. On the other hand, no reduction of m-NT occurs in the reaction mixture containing 0.5% Pt/A in the dark under Ar which confirms that 0.5% Pt/A is not able to catalyze the simple dark dehydrogenation of the alcohol thus resulting in a transfer of the hydrogenation reaction to the nitro group.

As can be seen from Table 2 (entries 1, 3, 5, and 7) the selectivity towards the mono N-alkylated product (4a) is affected by the type of TiO$_2$. The best selectivity was obtained employing 0.5% Pt/A. This can be explained by the activity of anatase to produce a higher amount of the imine (2a) as previously discussed. The production of the mono-N-alkylated product (4a) is a result of the hydrogenation of this imine catalyzed by the Pt nanoparticles deposited on the surface of TiO$_2$. It is noteworthy that H$_2$ can reduce the imine at the Pt surface even in the dark as confirmed by the reaction of the aniline (2a) with acetaldehyde in EtOH under an H$_2$ atmosphere for 2 h in the presence of 0.5% Pt/A while this reaction does not occur on bare TiO$_2$. In the case of Pt/P25, the presence of the co-catalyst, Pt, changes the reaction pathway from cyclization of 2a (step 3) to its hydrogenation to form 4a (step 3′) instead. The ATR-FTIR measurements (see S1, ESI†) showed that the deposition of Pt on the surface of P25 does not affect the Lewis acid sites on its surface. However, the weak peak at 1640 cm^{-1} corresponding to the Brønsted acid sites disappeared upon platinization of the surface.

Effect of the loaded amount of Pt and the platinization method

The data obtained from UV(A) illumination of an ethanolic solution of m-NT in the presence of Hombikat UV100 loaded with 0.3, 0.5, and 1.0 wt% Pt are given in Table 2 (entries 1, 9, and 11). Table 2 (entries 13 and 14) also shows the selectivity of the products obtained upon employing Pt/TiO$_2$ which was prepared by the mixing of solids method. It becomes obvious from these data that the amount of platinum, as well as the platinization method, plays an important role in the selectivity of the products especially the mono N-alkylated compound.

The selectivity toward 4a increases from 50% to 80% when the Pt loading increases from 0.3% to 1.0%. Pt sites significantly affect the condensation reaction of 1a with the photocatalytically generated acetaldehyde (step 2 in Scheme 2). The complete reduction of one nitro group to an amino group requires six electrons, i.e., whichever photocatalyst is used. This means that at least three molecules of alcohol will simultaneously be oxidized to the corresponding aldehyde considering the current doubling effect.[36] Thus, an excess amount of aldehyde, in relation to aniline, will be in the reaction mixture. The condensation of amines with aldehydes to form imines (step 2) is an equilibrium reaction, thus, the hydrogenation of the imine to 4a (step 3′) will shift the equilibrium
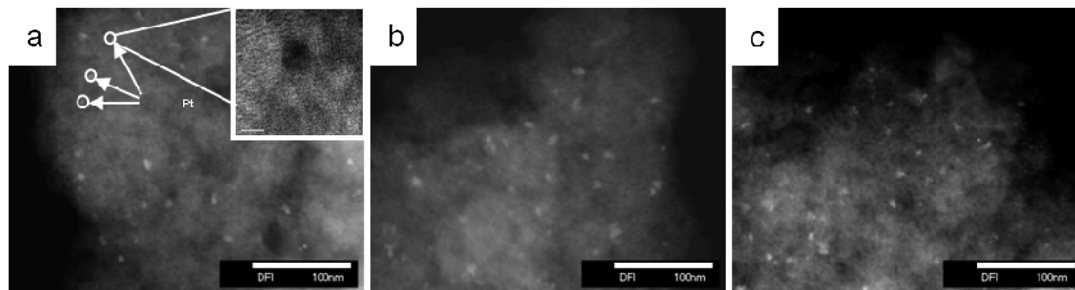
Fig. 3 TEM images of Hombikat UV100 samples with different amounts of Pt/TiO$_2$: (a) 0.3 wt%, (b) 0.5 wt%, and (c) 1.0 wt%. (a, inset) HRTEM image of 0.3 wt% Pt/TiO$_2$.

towards the complete consumption of **1a** to produce **4a**. Increasing the Pt-loading improves the catalytic efficiency for the hydrogenation of the C=N moiety hence increasing the yield of **4a**. The distribution of the Pt nanoparticles on the TiO$_2$ surface should have a decisive effect on the hydrogenation of **2a** to **4a**.

Dark-field TEM images of Pt/A (Fig. 3) clearly show that the Pt nanoparticles are well dispersed exhibiting particle diameters between 3 and 10 nm. However, no clear change in the particle size has been determined upon changing the loaded amounts of platinum. A theoretical calculation for the change in the particle size (see the Experimental part) predicts that when the amount of Pt is decreased from 1.0% *via* 0.5% to 0.3%, the particle size should change from 5 nm *via* 3.9 nm to 3.3 nm. However, these small changes cannot be clearly recognized from the TEM images. Interestingly, the calculations reveal that at a Pt-loading of 1% the ratio between the number of Pt particles and TiO$_2$ particles is approx. 1 : 270. Consequently, only a few of the TiO$_2$ particles will actually have direct contact with a Pt particle even at higher Pt loading (0.5% and 1.0%). Hence, photogenerated charge carriers, *e.g.*, electrons, need to move through the network of TiO$_2$ particles following the so-called antenna mechanism[37,38] to reach the Pt particles. Thus, it is not really clear whether the increase in the efficiency by increasing the amount of Pt-loading is due to an increase in the number of platinum islands deposited on the TiO$_2$ surface or to the growth of the individual platinum particles upon increasing the amount of H$_2$PtCl$_4$ during the catalyst preparation. However, in both cases increasing the loaded amount of Pt leads to an increase in the total surface area of Pt which, in turn, increases the efficiency of (**2a**) hydrogenation.

Shiraishi *et al.*[21] suggested that TiO$_2$ with higher Pt loading produces a larger amount of H$^+$ upon photocatalytic oxidation of benzyl alcohol in the presence of aromatic amines. These H$^+$ are not only reduced on the Pt surface but also react with the surface –OH groups on TiO$_2$, producing the Brønsted acid site (Ti–OH$_2^+$). Keeping in mind the effect of the Brønsted acid site on the fate of **2a**, we expected an increase in the yield of **3a** upon increasing the loaded amount of Pt. However, this was not the case; the selectivity towards **3a** decreased while the selectivity towards **4a** increased upon increasing the Pt amount. This can be explained by assuming that the hydrogenation rate
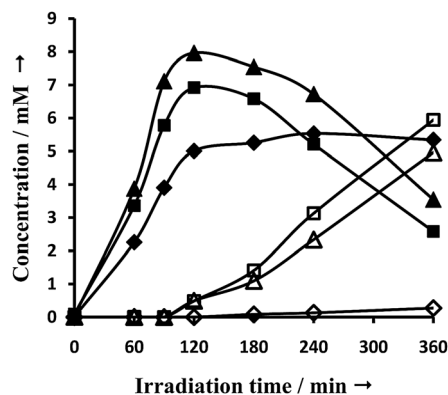

Fig. 4 Time-dependent change in the concentrations of (**4a**) (filled symbols) and NET (empty symbols) in the presence of: (0.3 wt%)Pt/A (◆), (0.5 wt%)Pt/A (■), and (1 wt%)Pt/A (▲).

of **2a** over Pt sites is higher than its cyclization rate over the Brønsted acid sites. Moreover, purging of Ar during the illumination of the reaction mixture (entries 21 and 22 in Table 2) to remove the liberated H$_2$ during the reaction was not sufficient to switch the reaction pathway from step 3′ to step 3. This indicates that the hydrogenation of **2a** occurs with H atoms adsorbed on the Pt site before they react with another H atom to generate H$_2$. On the other hand, it is clearly seen from Fig. 4 that the first N-alkylation reaction of **2a** to produce *N*-alkyl arylamine (**4a**) occurs faster over 1% Pt/A than over 0.5% Pt/A while the opposite was observed for the N-alkylation of **4a** to generate the *N,N*-dialkyl arylamine (**5a**); which is reflected in the selectivity of 1% Pt/A towards the mono N-alkylation reaction.

Effect of the platinization method

As can be noticed from the data presented in Table 2 (entries 13 and 14), colloidal Pt loaded onto Hombikat UV-100 is not as selective as that prepared by the photodeposition method. Although a complete conversion of *m*-NT occurred within 120 min, less than 10% selectivity for the formation of **4a** was obtained. Obviously, the type of interaction between Pt and TiO$_2$ also plays an important role in the activity of Pt as a hydrogenation catalyst. One explanation may be that the available surface of the platinum in the Pt/TiO$_2$, prepared photocatalytically, is higher than that of the Pt/TiO$_2$ prepared

by the mixing of solids method. In Pt/TiO$_2$ prepared by mixing of colloidal Pt with TiO$_2$, the Pt particles should rather be surrounded by TiO$_2$ particles which may reduce the available surface of Pt particles compared with their surface in the case of the photocatalytic deposition method. As was explained previously, Pt sites play an important role in both the condensation reaction of **1a** with the aldehyde and the hydrogenation reaction of the imine (**2a**).

Influence of light intensity and illumination time

The effect of the light intensity on both the conversion of the nitroaromatic compound and the selectivity of the products is illustrated in Table 2. It can be seen from these data (entries 15–20) that the photocatalytic conversion of *m*-NT, using (0.5 wt%) Pt/A, is still highly selective towards the formation of the mono N-alkylated product (**4a**) even when lower light intensities are used. It is obvious from these data that the reduction rate of the nitro compound decreased upon decreasing the light intensity. On the other side, more time was needed to attain the maximum yield of **4a**, while its selectivity was not significantly affected by the employed light intensity. Thus, even at lower light intensities which reduce the rate of H$_2$ production, step 3′ is preferred over step 3 in the presence of Pt as a co-catalyst.

On the other hand, prolonged illumination time will lead, in all cases, to the reductive alkylation of the produced **4a** by the photocatalytically generated acetaldehyde (step 4 in Scheme 2). This reaction step will involve the intermediate formation of the *N,N*-disubstituted hemiaminal. The latter can suffer, under the reductive conditions of this reaction, hydrogenolysis to produce the N,N-dialkylated product.[39]

N-alkylation reactions of various nitroaromatic compounds by different alcohols

In order to evaluate the general applicability of this photocatalytic N-alkylation method, various types of nitroaromatic compounds as well as different alcohols were studied. As can be seen from Table 3 the photocatalytic N-alkylation was successfully achieved in most cases with a moderate to a very good isolated yield.

However, the time required to achieve a complete conversion of the *m*-NT increases upon increasing the length of the aliphatic chain of the alcohol. This can be explained by the difference in the alcohol properties, such as viscosity, polarity, polarisability, and reduction potential. A similar effect of the alcohol parameters has been reported previously by Brezova *et al.*[40] They observed that the solvent viscosity significantly influenced the rate of 4-nitrophenol photoreduction on TiO$_2$ and a linear dependence was obtained, whereas, the rate of photocatalytic reduction increased with increasing polarity of the alcohol. On the other side, only trace amounts of the mono N-alkylated products were produced when branched or aromatic alcohols were used, whereas the main products under these reaction conditions were the imines in the case of 3-methyl-butanol or benzyl alcohol or even the aniline in the case of iso-propanol (entries 4–6 in Table 3). This shows that

steps 2–4 in Scheme 1 are indeed affected by the steric structure of the reacted alcohol. On the other hand, it can be seen from the data presented in Table 3 that the position of the methyl group in the nitro aromatic compound and its number do not affect the reaction sequence, *i.e.*, in all cases the mono N-alkylated products were obtained in very good yields (entries 7–10 in Table 2). Interestingly, *N*-ethyl-*m*-ethyl-benzene was obtained when *m*-nitrostyrene was used as a substrate (entry 10 in Table 3), which means that Pt/TiO$_2$ is not only able to photocatalytically hydrogenate the C=N double bond but also the C=C bond.

An overview of the suggested reaction mechanism of the photocatalytic conversion of the nitro aromatic compounds is given in Scheme 3.

Different transformations in this "one pot" system can be achieved by employing both the photocatalytic and the catalytic action of TiO$_2$ or Pt/TiO$_2$: the oxidation of the alcohol to the corresponding aldehyde consuming the photogenerated valence band holes of the illuminated TiO$_2$, the reduction of the nitro group of the nitroaromatic compound to an amino group either by the photogenerated conduction band electrons or through electrons initially trapped at the Pt deposits on the semiconductor's surface, and, subsequently, the condensation of the aldehyde and the amino compound to produce the imine. This imine can thereafter undergo one of the following reactions: hydrolysis to reproduce the starting amine, such as in the case of bare rutile, cyclization reaction when a Brønsted acid is present in the reaction media which is the case of P25, or hydrogenation to the corresponding secondary and tertiary amine when the TiO$_2$ is modified with Pt nanoparticles.
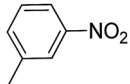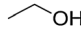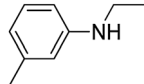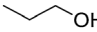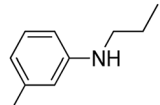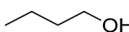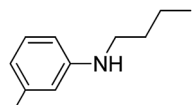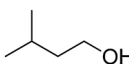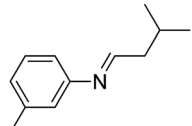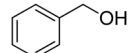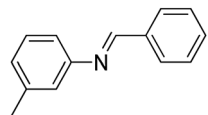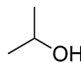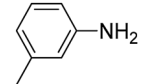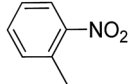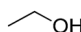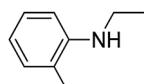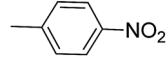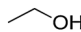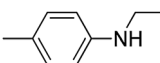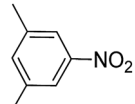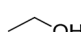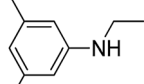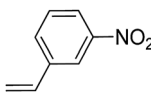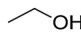
Conclusions

The photocatalytic conversion of nitro aromatic compounds in alcoholic suspensions of different types of TiO$_2$ or platinized TiO$_2$ under different conditions was examined and the following conclusions were drawn:

(1) The surface properties of the photocatalyst play an important role in the reaction pathway and strongly affect the selectivity of the products. The poor acidity of the rutile modification of titanium dioxide can explain the selectivity of the photocatalytic conversion of *m*-NT towards the primary amine. The catalytic con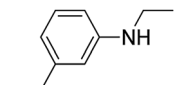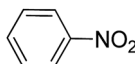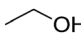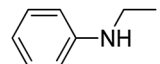densation of the photocatalytically produced aldehyde and amine occurs on the Lewis acid site on anatase TiO$_2$ to produce the corresponding imine. In the case of P25 the imine, which is produced on the Lewis acid sites, can suffer a cyclization reaction to yield the corresponding quinoline over the Brønsted acid sites that are also located on the TiO$_2$ surface.

(2) The presence of the co-catalyst, Pt, directs the photocatalytic reaction towards N-alkylation and N,N-dialkylation using any of the TiO$_2$ types. The platinized Hombikat UV100 shows the highest selectivity towards the mono N-alkylation reaction. The hydrogenation of the imine is considered to be the rate limiting, *i.e.*, the controlling step of the process forming the mono N-alkylated product. This hydrogenation

**Table 3** Photocatalytic N-alkylation of nitroaromatic compounds with alcohols over 1% Pt/TiO$_2$[a]

Entry	Nitroaromatic compound	Alcohol	Product	t^b (min)	Yield[c] (%) GC	is
1				150	90	85
2				180	100	91
3				240	83	80
4				360	91	d
5[d]				480	94	92
6				180	99	e
7				150	93	84
8				120	90	75
9				120	83	80
10				300	72	53
11				150	79	54

[a] Reaction conditions: 0.4 mmol nitroaromatic compound, 40 ml alcohol, 0.1 g 1% Pt/TiO$_2$, 25 °C, under Ar. [b] Illumination time needed to achieve 100% conversion of the nitroaromatic compound. [c] Yields were based on 100% nitroaromatic compound consumption. GC refers to the yields determined by GC analysis while is refers to the isolated yields. [d] 4 mmol of benzyl alcohol was dissolved in 40 ml MeCN. [e] Not isolated.

takes place on the surface of the Pt nanoparticles with a higher Pt loading resulting in a higher selectivity towards the mono N-alkylated product. Moreover, the catalysts prepared using the photodeposition method were found to be more active and selective than those obtained from the mixing of solids method. Controlling the light intensity as well as the illumination time will influence the selectivity of the formation of the mono N-alkylated product by determining the reaction conditions.

(3) The photocatalytic mono N-alkylation reaction of different nitro aromatic compounds with different alcohols can be successfully performed with a good yield indicating that this photocatalytic system can be applied for the commercial production of such valuable products.

This journal is © the Owner Societies 2013

Phys. Chem. Chem. Phys., 2013, **15**, 2992–3002 | **2999**
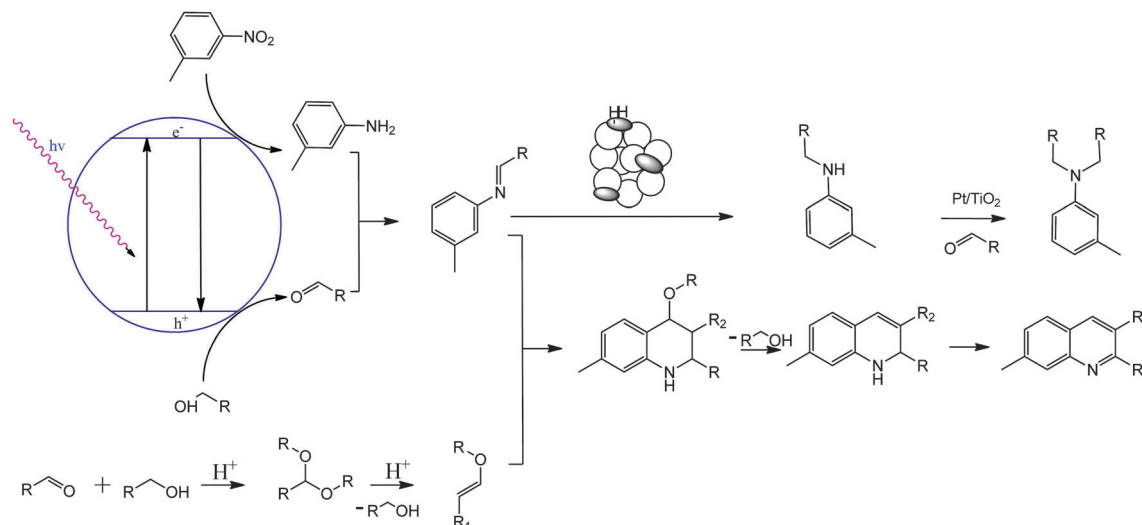
Scheme 3 Proposed mechanism for the one-pot photocatalytic conversion of *m*-nitrotoluene promoted by a TiO_2 or Pt/TiO_2 catalyst under photoirradiation.

Experimental

Sachtleben Hombikat UV100, Crystal Global R34 and Evonik Aeroxide P25 were used as received as genereous gifts from the respective companies. Mesoporous titania was prepared according to a procedure given in ref. 38, which yields photocatalyst materials with a hexagonal mesostructure.

Two methods were used to prepare Pt/TiO_2: the photocatalytic deposition method and the mixing of solids method, respectively.

Photocatalytic deposition

$Pt(x)/TiO_2$ samples, containing different platinum loadings $[x \text{ (wt%)} = 100 \times m(Pt)/[m(TiO_2) + m(Pt)]; x = 0.3, 0.5, 1.0]$, were prepared by a photodeposition method.[41] In a typical experiment, 0.5 g of the TiO_2 powder were suspended in 100 ml of deionized water and purged with argon for 30 min to remove dissolved O_2. H_2PtCl_6 of the desired concentration was added to the suspension and the mixture was irradiated from the top for 1 h with UVA light using a Philips CLEO lamp (3 mW cm^{-2}) and then 1 ml of methanol was added to the suspension and kept under illumination overnight. Removal of the reaction solution by centrifugation, followed by repeated washing of the powder with distilled water, and finally drying at 80 °C for 24 h yielded a gray solid.

Mixing of solids

Colloidal Pt was prepared by reduction of H_2PtCl_6 with sodium citrate.[42] Excess ions in the resulting colloidal suspension were removed with an ion exchange resin (Amberlite MBl) until a specific conductivity of *ca.* 3 μS cm^{-1} was reached. Pt loaded TiO_2 (0.5 wt%) was prepared by suspending TiO_2 in deionized water followed by the addition of the desired amount of the as-prepared colloidal Pt under continuous magnetic stirring overnight. After evaporation under vacuum at room temperature,

a grayish powder was obtained. The obtained powder was dried at 80 °C overnight.

Sample characterization

The acidic sites on the surface of TiO_2 powders were investigated by FTIR spectroscopy of adsorbed pyridine. TiO_2 powders were heated to 120 °C for 24 h to remove adsorbed water from their surfaces. Subsequently, the samples were transferred to a desiccator saturated with pyridine vapor and stored in the dark for 24 h at room temperature. At the end of the saturation process, the samples were flushed with N_2 flow for 1 h to remove the weakly adsorbed pyridine molecules.

FTIR spectra were recorded on a BRUKER FRA 106 instrument using KBr pressed powder discs. Each sample of TiO_2 powders (10 mg) was mixed with 190 mg of spectroscopically pure dry KBr and pressed into disks before its spectrum was recorded.

TEM and HRTEM measurements were carried out on a Field-Emission Transmission Electron Microscope of the type JEM-2100F-UHR (JEOL Ltd., Tokyo, Japan) equipped with a Gatan GIF 2001 energy filter and a 1k CCD camera. HRTEM was performed at 200 kV with an ultrahigh resolution pole piece (CS = 0.5 mm), which provides a point-resolution better than 0.19 nm.

The theoretical calculation of the change in Pt particle size was carried out as follows: assuming that Pt nanoparticles are semi-sphere like, the volume of one 5 nm Pt nanoparticle (1 wt% Pt) is 32.23 nm^3. Considering that the mass density of platinum is 21.4 g cm^{-3}, the average weight of one Pt nanoparticle is derived to be *ca.* 6.9×10^{-19} g. Likewise, the mass density of anatase TiO_2 is 3.894 g cm^{-3}, so the average weight of a 5 nm TiO_2 nanoparticle is *ca.* 2.55×10^{-19} g. Therefore, the average weight ratio between Pt and TiO_2 nanoparticles is obtained: $W(Pt)/W(TiO_2) = 2.7$. The difference in the Pt particle size as the loaded Pt amount differs was calculated assuming that the number of Pt particles is constant (14×10^{17} particles).

Single-point standard BET surface area measurements were carried out employing a Micromeritics AutoMate 23 instrument. A gas mixture of 30% nitrogen and 70% helium was used for the adsorption determinations. The TiO_2 samples were previously heated to 120 °C for approximately 1 h to remove adsorbed water.

Photoreaction procedure

In a typical experimental run 25 mg of the photocatalyst was suspended in 10 cm³ of an ethanolic solution (Roth) containing 100 μmol of m-nitrotoluene (Aldrich, 99%). The reaction was carried out in a double jacket Duran glass reactor with a total volume of 40 cm³ which was irradiated from the outside using an Osram XBO 1000 W Xenon lamp in a Mueller LAX 1000 lamp housing under magnetic stirring at 25 °C. A 10 cm water bath and a WG 320 nm filter were used to cut off the IR and short wavelength UV light, respectively. Before illumination, the reactor was placed in a sonicator for 3 min and then purged with Ar until no N_2 and O_2 were detected by gas chromatography (Shimadzu 8A, TCD detector) in the headspace above the solution. The reactant and the products were analyzed qualitatively and quantitatively at different illumination times, after removing the semiconductor particles through filtration (0.20 μm filter) from the irradiated mixture, by GC/MS and GC/FID, respectively. For GC/MS analysis, a Shimadzu gas chromatograph and mass spectrometer (Shimadzu GC/MS-QP 5000) equipped with a 30 m Rxi-5ms (d = 0.32 mm) capillary column was used. Operating temperatures programmed: injection temperature 305 °C, oven temperature 120 °C (hold 2 min) from 120 °C to 280 °C at a rate of 10 °C min⁻¹, 280 °C (hold 15 min) in splitless mode, injection volume was 3.0 μl with helium as a carrier gas. A Shimadzu GC 2010 equipped with a Rtx-5 (d = 0.25 mm) capillary column and an FID detector were used to determine the concentration of the reactant and of the products. Operating temperatures programmed: injection temperature 250 °C, oven temperature 70 °C (hold 2 min) from 70 °C to 280 °C at a rate of 10 °C min⁻¹, in splitless mode. Injection volume was 2.0 μl with nitrogen as the carrier gas. The concentrations of the substrate as well as the products were determined based on calibration curves prepared with authentic standards (m-toluidine; Aldrich 99%, N-ethyl-m-toluidine; Fluka 98%, N,N-diethyl-m-toluidine; Acros 99%, and 2,7-dimethylquinoline; Aldrich 99%).

The produced H_2 was also analyzed in the headspace above the reaction mixture during the illumination using a gas chromatograph (Shimadzu 8A) equipped with a Mole Sieve 5A column and a TCD detector using Ar as carrier gas. Column and detection temperatures were 60 °C and 150 °C, respectively.

In order to isolate the N-alkylated products employing (1%)Pt/TiO_2 as a photocatalyst, a double jacket Duran glass reactor was fed with 40 ml of the reaction mixture and irradiated from the outside by a 500 W mercury medium-pressure lamp (Heraeus TQ 718 Z4) with an UV(A) light intensity of 20 mW cm⁻². After the complete consumption of the nitro aromatic compound, as was detected by the GC analysis, the catalyst was removed by filtration followed by evaporation of

the solvent by a rotavapor. The products were purified by silica gel column chromatography with n-hexane : ethyl acetate 8 : 2 (v/v) as an eluent. The structures of the isolated products were confirmed by both GC-MS analysis and ¹H NMR and ¹³C NMR measurements recorded in $CDCl_3$.

References

1 B. Ohtani, B. Pal and S. Ikeda, *Catal. Surv. Asia*, 2003, **7**, 165–176.
2 G. Palmisano, V. Augugliaro, M. Pagliaro and L. Palmisano, *Chem. Commun.*, 2007, 3425–3437.
3 Y. Shiraishi and T. Hirai, *J. Photochem. Photobiol., C*, 2008, **9**, 157–170.
4 X. J. Lang, H. W. Ji, C. C. Chen, W. H. Ma and J. C. Zhao, *Angew. Chem., Int. Ed.*, 2011, **50**, 3934–3937.
5 K. H. Park, H. S. Joo, K. I. Ahn and K. Jun, *Tetrahedron Lett.*, 1995, **36**, 5943–5946.
6 H. C. Pehlivanugullari, E. Sumer and H. Kisch, *Res. Chem. Intermed.*, 2007, **33**, 297–309.
7 L. Cermenati, C. Richter and A. Albini, *Chem. Commun.*, 1998, 805–806.
8 A. Hakki, R. Dillert and D. Bahnemann, *Catal. Today*, 2009, **144**, 154–159.
9 T. Y. Zhang, L. Y. You and Y. L. Zhang, *Dyes Pigm.*, 2006, **68**, 95–100.
10 S. I. Nishimoto, B. Ohtani, T. Yoshikawa and T. Kagiya, *J. Am. Chem. Soc.*, 1983, **105**, 7180–7182.
11 M. Hopfner, H. Weiss, D. Meissner, F. W. Heinemann and H. Kisch, *Photochem. Photobiol. Sci.*, 2002, **1**, 696–703.
12 S. Marinkovic and N. Hoffmann, *Eur. J. Org. Chem.*, 2004, 3102–3107.
13 F. Mahdavi, T. C. Bruton and Y. Z. Li, *J. Org. Chem.*, 1993, **58**, 744–746.
14 J. L. Ferry and W. H. Glaze, *Langmuir*, 1998, **14**, 3551–3555.
15 H. Tada, T. Ishida, A. Takao, S. Ito, S. Mukhopadhyay, T. Akita, K. Tanaka and H. Kobayashi, *ChemPhysChem*, 2005, **6**, 1537–1543.
16 M. A. Fox, in *Electron Transfer in Chemistry*, ed. V. Balzani, Wiley-VCH Verlag GmbH, Weinheim, Germany, 2008, pp. 271–311.
17 W. Kemula and T. M. Krygowski, in *Encyclopedia of electrochemistry*, ed. A. J. Bard and H. E. Lund, M. Dekker, New York, 1979, pp. 77–130.

18 B. Ohtani, H. Osaki, S. Nishimoto and T. Kagiya, *J. Am. Chem. Soc.*, 1986, **108**, 308–310.

19 B. Ohtani, H. Osaki, S. Nishimoto and T. Kagiya, *Chem. Lett.*, 1985, 1075–1078.

20 M. A. Valenzuela, O. Rios-Berny, S. O. Flores and I. Cordova, *Tetrahedron Lett.*, 2010, **51**, 2730–2733.

21 Y. Shiraishi, M. Ikeda, D. Tsukamoto, S. Tanaka and T. Hirai, *Chem. Commun.*, 2011, **47**, 4811–4813.

22 K. Selvam and M. Swaminathan, *Catal. Commun.*, 2011, **12**, 389–393.

23 K. Selvam and M. Swaminathan, *Tetrahedron Lett.*, 2010, **51**, 4911–4914.

24 B. Ohtani, Y. Goto, S. Nishimoto and T. Inui, *J. Chem. Soc., Faraday Trans.*, 1996, **92**, 4291–4295.

25 Y. Matsushita, N. Ohba, T. Suzuki and T. Ichimura, *Catal. Today*, 2008, **132**, 153–158.

26 Y. Matsushita, N. Ohba, S. Kumada, K. Sakeda, T. Suzuki and T. Ichimura, *Chem. Eng. J.*, 2008, **135**, S303–S308.

27 K. Selvam and M. Swaminathan, *J. Mol. Catal. A: Chem.*, 2011, **351**, 52–61.

28 K. Selvam and M. Swaminathan, *Bull. Chem. Soc. Jpn.*, 2011, **84**, 953–959.

29 I. X. Green, C. Buda, Z. Zhang, M. Neurock and J. T. Yates, *J. Phys. Chem. C*, 2010, **114**, 16649–16659.

30 S. Kim, X. Y. Wang, C. Buda, M. Neurock, O. B. Koper and J. T. Yates, *J. Phys. Chem. C*, 2009, **113**, 2219–2227.

31 X. C. Wang, J. C. Yu, P. Liu, X. X. Wang, W. Y. Su and X. Z. Fu, *J. Photochem. Photobiol., A*, 2006, **179**, 339–347.

32 T. Bezrodna, G. Puchkovska, V. Shimanovska, I. Chashechnikova, T. Khalyavka and J. Baran, *Appl. Surf. Sci.*, 2003, **214**, 222–231.

33 A. P. Kulkarni and D. S. Muggli, *Appl. Catal., A*, 2006, **302**, 274–282.

34 G. Martra, *Appl. Catal., A*, 2000, **200**, 275–285.

35 X. Geng, S. S. Li, X. Q. Bian, Z. Y. Xie and C. D. Wang, *ARKIVOC*, 2008, 50–57.

36 C. Y. Wang, R. Pagel, D. W. Bahnemann and J. K. Dohrmann, *J. Phys. Chem. B*, 2004, **108**, 14082–14092.

37 C. Y. Wang, R. Pagel, J. K. Dohrmann and D. W. Bahnemann, *C. R. Chim.*, 2006, **9**, 761–773.

38 A. A. Ismail, D. W. Bahnemann, L. Robben, V. Yarovyi and M. Wark, *Chem. Mater.*, 2010, **22**, 108–116.

39 J. March, *Advanced Organic Chemistry*, Wiley, 1985.

40 V. Brezova, A. Blazkova, I. Surina and B. Havlinova, *J. Photochem. Photobiol., A*, 1997, **107**, 233–237.

41 B. Kraeutler and A. J. Bard, *J. Am. Chem. Soc.*, 1978, **100**, 4317–4318.

42 D. Bahnemann, A. Henglein, J. Lilie and L. Spanhel, *J. Phys. Chem.*, 1984, **88**, 709–711.